CHEMISTRY
A European Journal

Supporting Information

Self-Assembled, Fluorine-Rich Porous Organic Polymers: A Class of Mechanically Stiff and Hydrophobic Materials

Soumya Mukherjee+,[a] Zhixin Zeng+,[b] Mandar M. Shirolkar,[c, d] Partha Samanta,[a] Abhijeet K. Chaudhari,[b] Jin-Chong Tan,*[b] and Sujit K. Ghosh*[a, e]

chem_201802200_sm_miscellaneous_information.pdf

Experimental Section:

Materials: All the reagents and solvents were commercially available and used without further purification.

Synthesis of precursor L'

3,5-bis(trifluoromethyl)aniline (5 g, 22 mmol), 4- fluorobenzonitrile (6.1 g, 50 mmol) and cesium fluoride (~ 10 g, 66 mmol) were refluxed at 170 °C in *N,N*-dimethylformamide (DMF) (250 mL) over 48 h. After cooling the reaction mixture to r.t., it was poured into ~ 500 mL ice-cold water, which yielded light brown coloured precipitation. This was filtered under vacuum, washed well with water, and this crude product was recrystallized from methanol to obtain the brown coloured crystalline precursor L' (Fig. S1). Yield: 7.6 g, ~ 80%. ^{1}H NMR (400 MHz, DMSO-d^6) (Fig. S3): δ 7.6 (m, 5H), 7.5 (s, 2H), 7.1 (m, 4H); ^{13}C NMR (100 MHz, $CDCl_3$) (Fig. S4): 149.4, 147.2, 134.4, 134.2, 133.9, 125.2, 124.4, 119.0, 118.5, 108.4; HRMS (Fig. S2): Calc. for $C_{22}H_{11}F_6N_3$ $[M+H]^+$: 432.0930; Found: 432.0930. Elemental Analysis: Anal. Calcd for $C_{22}H_{11}F_6N_3$: C, 61.26; H, 2.57; N, 9.74. Found: C, 61.19; H, 2.60; N, 9.69.

Synthesis of precursor L''

2,5-bis(trifluoromethyl)aniline (5 g, 22 mmol), 4- fluorobenzonitrile (6.1 g, 50 mmol) and cesium fluoride (~ 10 g, 66 mmol) were refluxed at 165 °C in N, N-dimethylformamide (DMF) (250 mL) for 72 h. After cooling the reaction mixture to r.t., it was poured into ~ 500 mL ice-cold water, which yielded yellow coloured precipitation. This was filtered under vacuum, washed well with water, and this crude product was recrystallized from methanol to obtain the yellow coloured crystalline precursor compound L" (Fig. S5). Yield: 6.9 g, ~ 73%. ^{1}H NMR (400 MHz, DMSO-d^6) (Fig. S7): δ 8.0 (d, J = 8.4 Hz, 1H), 7.8 (d, J = 8.4 Hz, 1H), 7.5 (m, 5H), 7.0 (m, 4H);

^{13}C NMR (100 MHz, $CDCl_3$) (Fig. S8): δ 149.3, 143.1, 133.6, 129.9, 129.5, 125.1, 122.3, 118.5, 106.8; HRMS (Fig. S6): Calc. for $C_{22}H_{11}F_6N_3$ $[M+H]^+$: 432.0930; Found: 432.0997. Elemental Analysis: Anal. Calcd for $C_{22}H_{11}F_6N_3$: C, 61.26; H, 2.57; N, 9.74. Found: C, 61.30; H, 2.69; N, 9.80.

Synthesis of FPOP-100

Trifluoromethanesulfonic acid (0.47 g, 3.12 mmol) in 10 mL of $CHCl_3$ was charged into a pre-dried 2-neck round bottom flask under N_2 atmosphere. The mixture was cooled to 273K and 4,4'-(3,5-bis(trifluoromethyl)phenylazanediyl)dibenzonitrile (L' , 500 mg, 1.16 mmol) in 55 mL of $CHCl_3$ was added into the solution dropwise over ~ 20 min. The mixture was stirred at 273K for another 2h before left overnight at room temperature. The solution turned dark brown, in which a red precipitate could be noticed. Then, the mixture was poured into ~ 250 mL of water containing 12 mL of ammonia solution and was stirred for 4h. The dark red precipitate was filtered and washed with water, ethanol, acetone and chloroform successively to yield bright red solid **FPOP-100** (372 mg; Inset of Fig. 1a). FT-IR (KBr, cm^{-1}): 1921, 1713, 1520, 1358, 1103, 849 (Fig. S24). Elemental analysis (%) of **FPOP-100**: found: C, 62.52; H, 3.00; N, 11.36.

Synthesis of FPOP-101

Similar procedure (with the same scale and equivalent ratios of reactants and solvents; difference being the use of L" [4,4'-(2,5-bis(trifluoromethyl)phenylazanediyl)dibenzo-nitrile] instead of its positional isomer L') as the aforementioned one (for **FPOP-100**) yielded **FPOP-101** as a dark brown solid (380 mg; Inset of Fig. 1b). FT-IR (KBr, cm^{-1}): 1936, 1728, 1512, 1110, 826 (Fig. S24). Elemental analysis (%) of **FPOP-100**: found: C, 63.48; H, 3.8; N, 11.28.

Synthesis of L_1, L_2 and L_3 and corresponding POPs (MPOP-100, MPOP-101, POP-100)

Procedures and the respective structural characterization data-sets for the non-fluorinated congeners (L_1: 4,4'-(3,5-dimethylphenylazanediyl)dibenzonitrile; L_2: 4,4'-(2,5-dimethylphenylazanediyl)dibenzonitrile; L_3: 4,4'-(phenylazanediyl)dibenzonitrile) and their corresponding POPs (**MPOP-100**, **MPOP-101** and **POP-100** respectively) have been elaborated in the supporting information file (Figures S9-S17).

Synthesis of L_1, L_2 and L_3 and corresponding POPs (MPOP-100, MPOP-101, POP-100)

Synthetic procedures and the respective structural characterization data-sets for the non-fluorinated congeners (L_1: 4,4'-(3,5-dimethylphenylazanediyl)dibenzonitrile; L_2: 4,4'-(2,5-dimethylphenylazanediyl)dibenzonitrile; L_3: 4,4'-(phenylazanediyl)dibenzonitrile) and their corresponding POPs (**MPOP-100**, **MPOP-101** and **POP-100** respectively) have been elaborated as following (additional data: Figures S9-S17 and S30-S31).

Synthesis of precursor L_1

3,5-dimethylaniline (2.5 g, 20.6 mmol), 4- fluorobenzonitrile (5.7 g, 47 mmol) and cesium fluoride (9.4 g, 62 mmol) were refluxed at 165 °C in *N*,*N*-dimethylformamide (DMF) (130 mL) for 72 h (Figure S9). After cooling the reaction mixture to r.t., it was poured into ~350 mL ice-cold water, which yielded dark yellow coloured precipitation. This was filtered under vacuum suction, washed well with water, and this crude product was recrystallized from methanol to obtain the bright yellow coloured crystalline precursor compound L_1 (Figure S9). Yield: 4.3 g, ~64%. ^{1}H NMR (270 MHz, $CDCl_3$) (Figure S10): δ 7.7 (t, $J = 2.4$ Hz, 4H), 7.5 (m, 4H), 6.9 (m, 1H), 6.7 (m, 2H), 2.2 (s, 6H); ^{13}C NMR (67.5 MHz, $CDCl_3$) (Figure S11): δ 150.2, 144.8, 140.2, 133.4, 128.4, 124.8, 122.8, 119.7, 108.0, 21.2. Elemental Analysis: Anal. Calcd for $C_{22}H_{17}N_3$: C, 81.71; H, 5.30; N, 12.99. Found: C, 82.01; H, 5.51; N, 13.24.

Synthesis of precursor L_2

2,5-dimethylaniline (2.5 g, 20.6 mmol), 4- fluorobenzonitrile (5.7 g, 47 mmol) and cesium fluoride (9.4 g, 62 mmol) were refluxed at 165 °C in *N*,*N*-dimethylformamide (DMF) (130 mL) for 48 h (Figure S12). After cooling the reaction mixture to r.t., it was poured into ~350 mL ice-cold water, which yielded black coloured precipitation. This was filtered under vacuum suction, washed well with water, and this crude product was recrystallized from methanol to obtain the dark brown coloured amorphous precursor compound L_2 (Figure S12). Yield: 3.9 g, ~58.5%. ^{1}H NMR (270 MHz, $CDCl_3$) (Figure S13): δ 7.7 (t, *J* = 2.4 Hz, 4H), 7.5 (m, 4H), 6.9 (m, 1H), 6.7 (m, 2H), 2.3 (s, 6H); ^{13}C NMR (67.5 MHz, $CDCl_3$) (Figure S14): δ 150.4, 140.3, 134.6, 133.5, 128.5, 124.9, 122.8, 119.8, 108.1, 21.3, 10.9. Elemental Analysis: Anal. Calcd for $C_{22}H_{17}N_3$: C, 81.71; H, 5.30; N, 12.99. Found: C, 82.04; H, 5.78; N, 12.86.

Synthesis of precursor L_3

Aniline (2.5 g, 27 mmol), 4- fluorobenzonitrile (7.44 g, 61.4 mmol) and cesium fluoride (12.3 g, 81 mmol) were refluxed at 165 °C in *N*,*N*-dimethylformamide (DMF) (130 mL) for 72 h (Figure S15). After cooling the reaction mixture to r.t., it was poured into ~350 mL ice-cold water, which yielded pale yellow coloured precipitation. This was filtered under vacuum suction, washed well with water, and this crude product was recrystallized from methanol to obtain the bright yellow coloured amorphous precursor compound L_3 (Figure S15). Yield: 5.1 g, ~64.4%. ^{1}H NMR (270 MHz, $CDCl_3$) (Figure S16): *δ* 7.7 (m, 4H), 7.5 (m, 2H), 7.1 (m, 5H), 7.0 (m, 1H), 6.7 (m, 1H); ^{13}C NMR (67.5 MHz, $CDCl_3$) (Figure S17): *δ* 150.2, 140.2, 134.4, 133.4, 128.4, 124.8, 122.6, 119.7, 105.4. Elemental Analysis: Anal. Calcd for $C_{20}H_{13}N_3$: C, 81.34; H, 4.44; N, 14.23. Found: C, 81.79; H, 4.95; N, 13.97.

Synthesis of MPOP-100

Trifluoromethanesulfonic acid (0.46 g, 3.1 mmol) in 10 mL of $CHCl_3$ was charged into a pre-dried 2-neck round bottom flask under N_2 atmosphere. The mixture was cooled to 273K and 4,4'-(3,5-dimethylphenylazanediyl)dibenzonitrile (L_1, 500 mg, 1.55 mmol) in 60 mL of $CHCl_3$ was added into the solution dropwise over ~20 min. The mixture was stirred at 273K for another 2h before left overnight at room temperature. The solution turned dark brown, in which a red precipitate could be noticed. Then, the mixture was poured into ~250 mL of water containing 12 mL of ammonia solution and was stirred for 4h. The dark red precipitate was filtered and washed with water, ethanol, acetone and chloroform successively to yield black powdered solid **MPOP-100** (315 mg; Figure S29). FT-IR (KBr, cm^{-1}) (Figure S30): 1695, 1574, 1499, 1418, 1358, 1222, 1172, 1126, 1082, 1023, 842. Elemental analysis (%) of **MPOP-100**: found: C, 65.74; H, 3.48; N, 10.98.

Synthesis of MPOP-101

Similar procedure (with the same scale and equivalent ratios of reactants and solvents; difference being the use of L_2 [4,4'-(2,5-dimethylphenylazanediyl)dibenzonitrile] instead of its positional isomer L_1) as the aforementioned one (for **MPOP-100**) yielded **MPOP-101** as a black powdered solid (295 mg; Figure S29). FT-IR (KBr, cm^{-1}) (Figure S30): 1692, 1572, 1500, 1420, 1360, 1223, 1170, 1125, 1084, 1024, 844. Elemental analysis (%) of **MPOP-101**: found: C, 66.34; H, 3.87; N, 11.05.

Synthesis of POP-100

Trifluoromethanesulfonic acid (0.51 g, 3.4 mmol) in 10 mL of $CHCl_3$ was charged into a pre-dried 2-neck round bottom flask under N_2 atmosphere. The mixture was cooled to 273K and 4,4'-(3,5-bis(trifluoromethyl)phenylazanediyl)dibenzonitrile (L' , 500 mg, 1.7 mmol) in 55 mL of $CHCl_3$ was added into the solution dropwise over ~20 min. The mixture was stirred at 273K for another 2h before left overnight at room temperature. The solution turned dark brown, in which a red precipitate could be noticed. Then, the mixture was poured into ~250 mL of water containing 12 mL of ammonia solution and was stirred for 4h. The dark red precipitate was filtered and washed with water, ethanol, acetone and chloroform successively to yield dark brown powdered solid **POP-100** (380 mg; Figure S29). FT-IR (KBr, cm^{-1}) (Figure S30): 1685, 1570, 1540, 1502, 1466, 1419, 1354, 1275, 1166, 1026, 886. Elemental analysis (%) of **POP-100**: found: C, 61.89; H, 3.97; N, 11.19.

Synthesis of Building Block L':

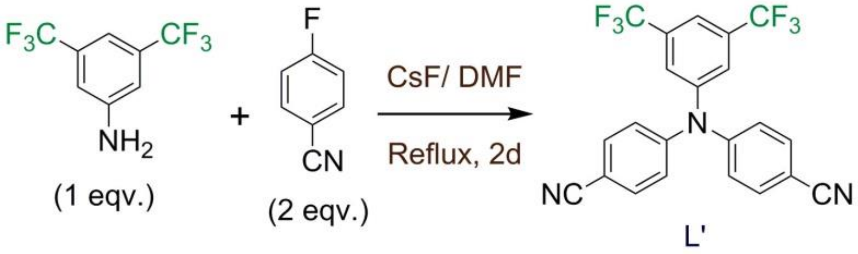

Figure S1: Synthesis protocol for the building block L'.

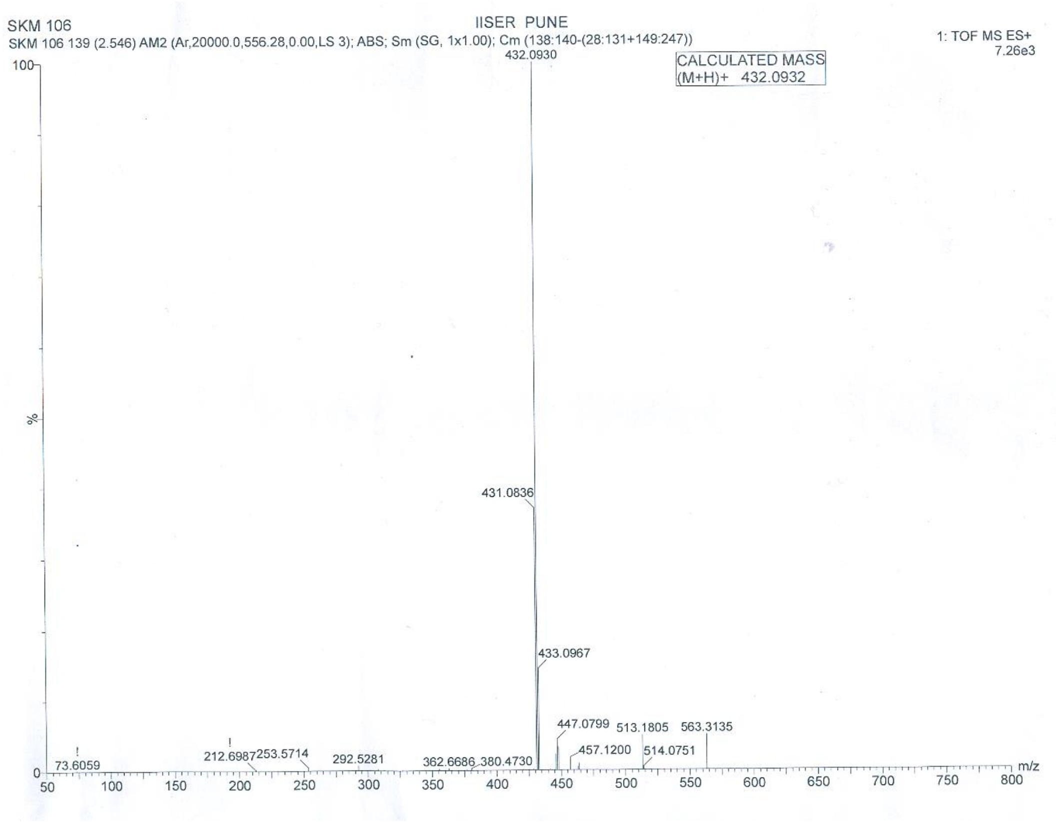

Figure S2: HRMS of building block L'.

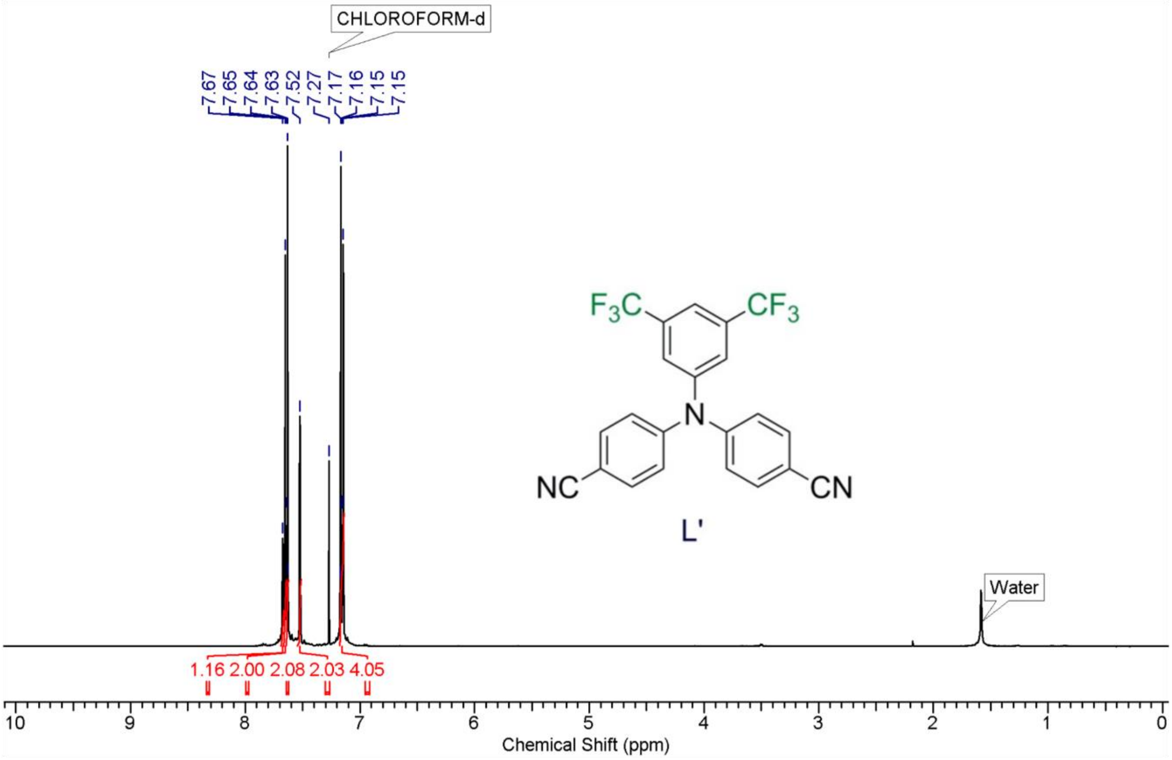

Figure S3: ^{1}H NMR of building block L'.

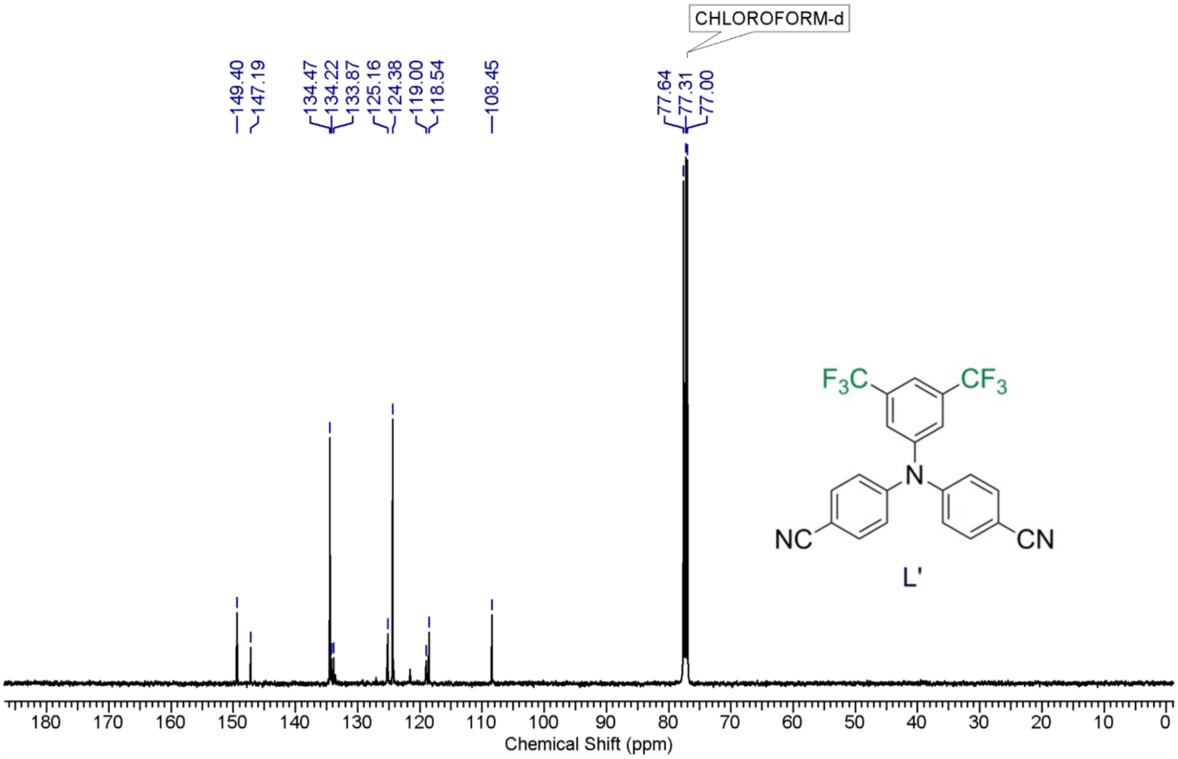

Figure S4: ^{13}C NMR of building block L'.

Synthesis of Building Block L'':

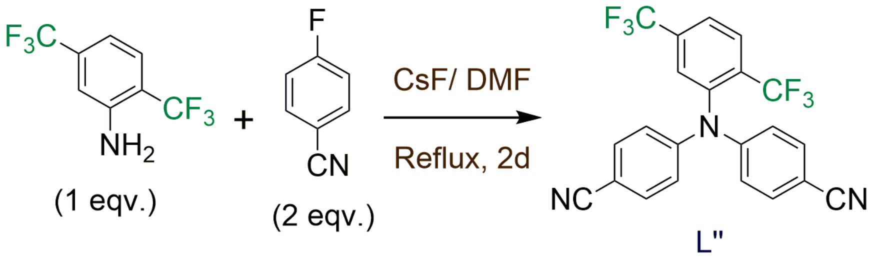

Figure S5: Synthesis protocol for the building block L''.

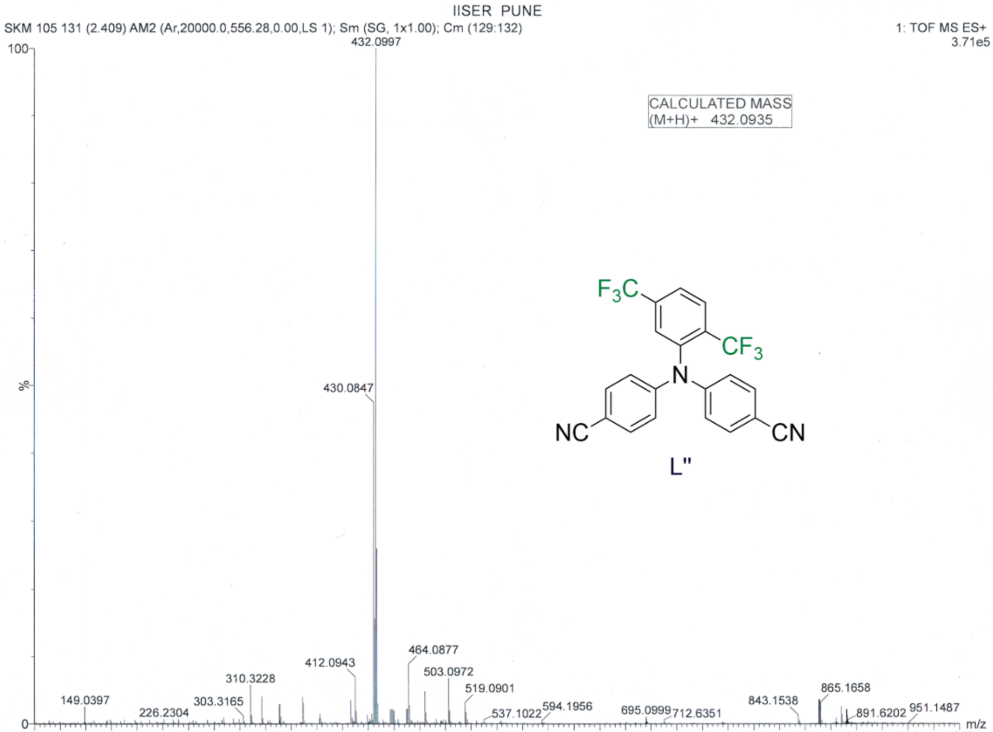

Figure S6: HRMS of building block L".

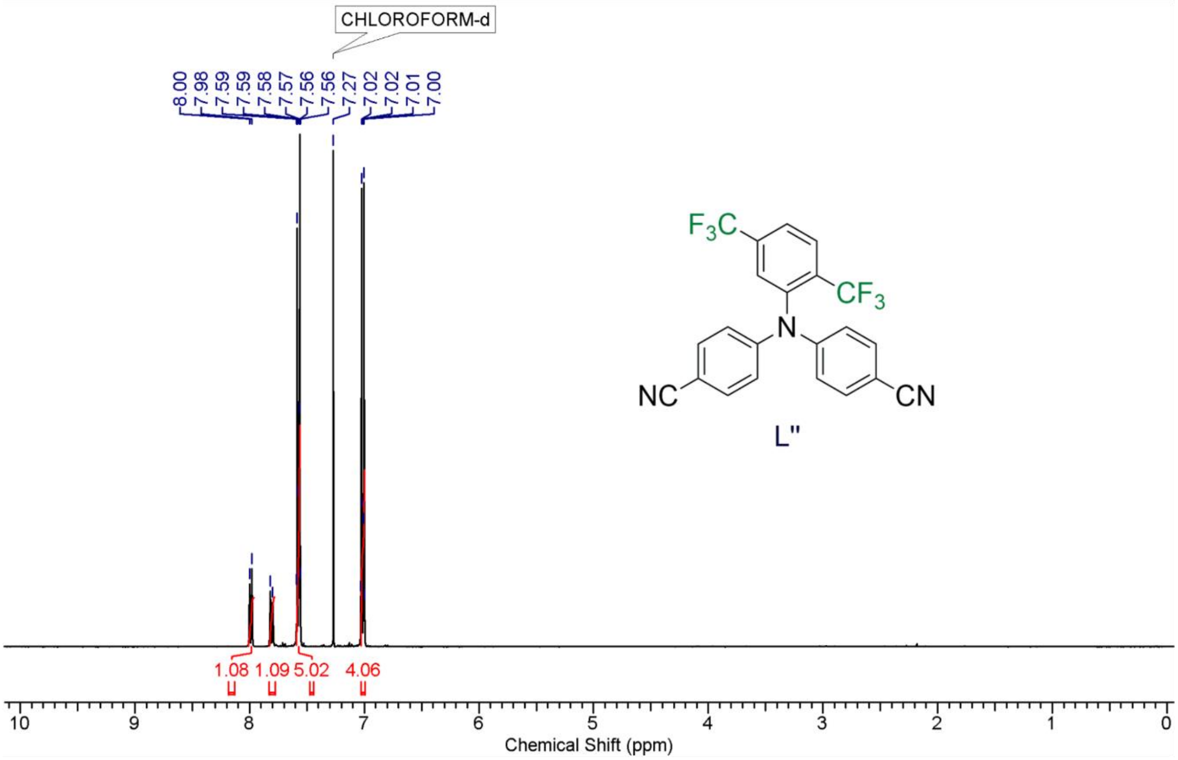

Figure S7: ^{1}H NMR of building block L".

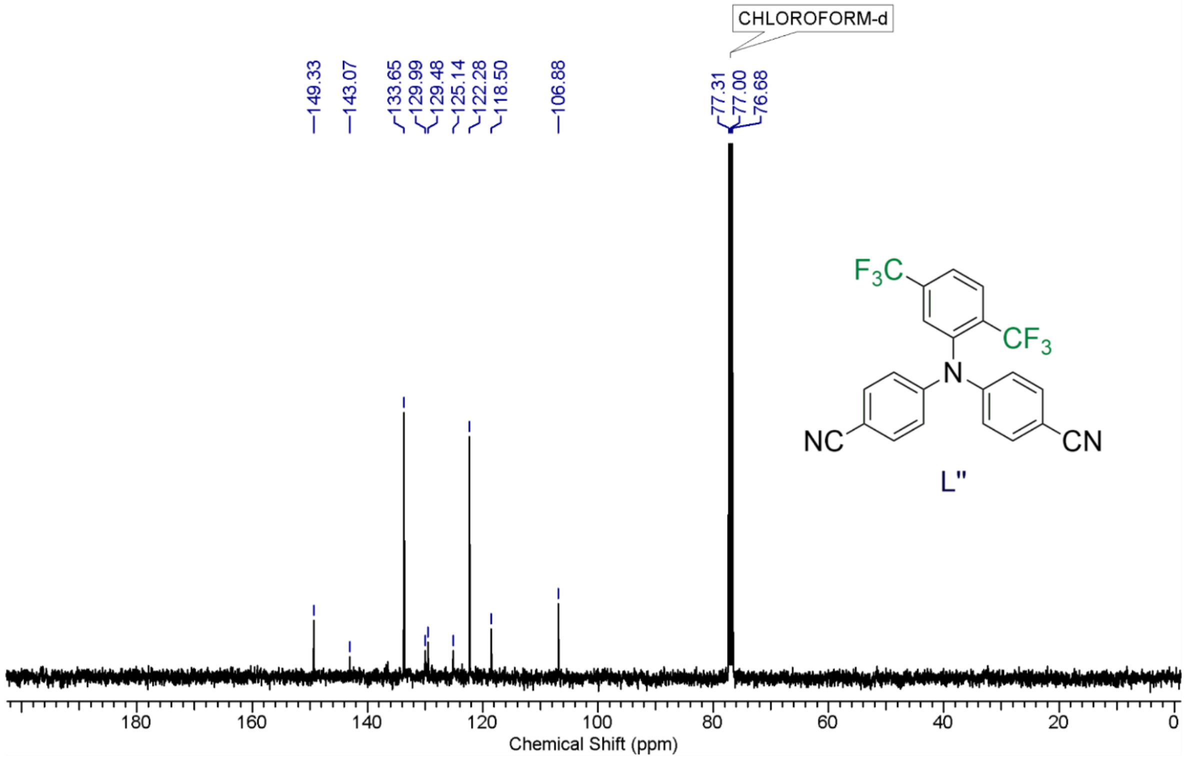

Figure S8: ^{13}C NMR of building block L".

Synthesis of Building Block L$_1$:

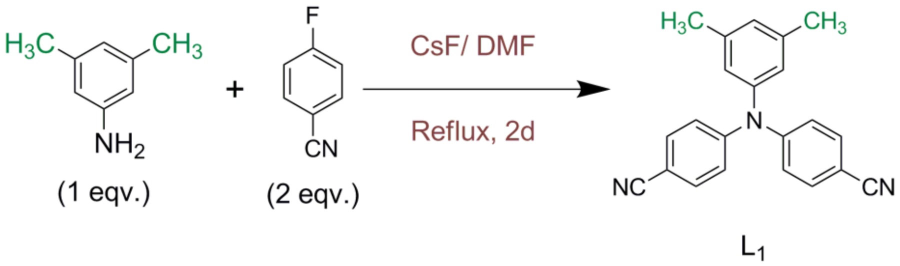

Figure S9: Synthesis protocol for the building block L$_1$.

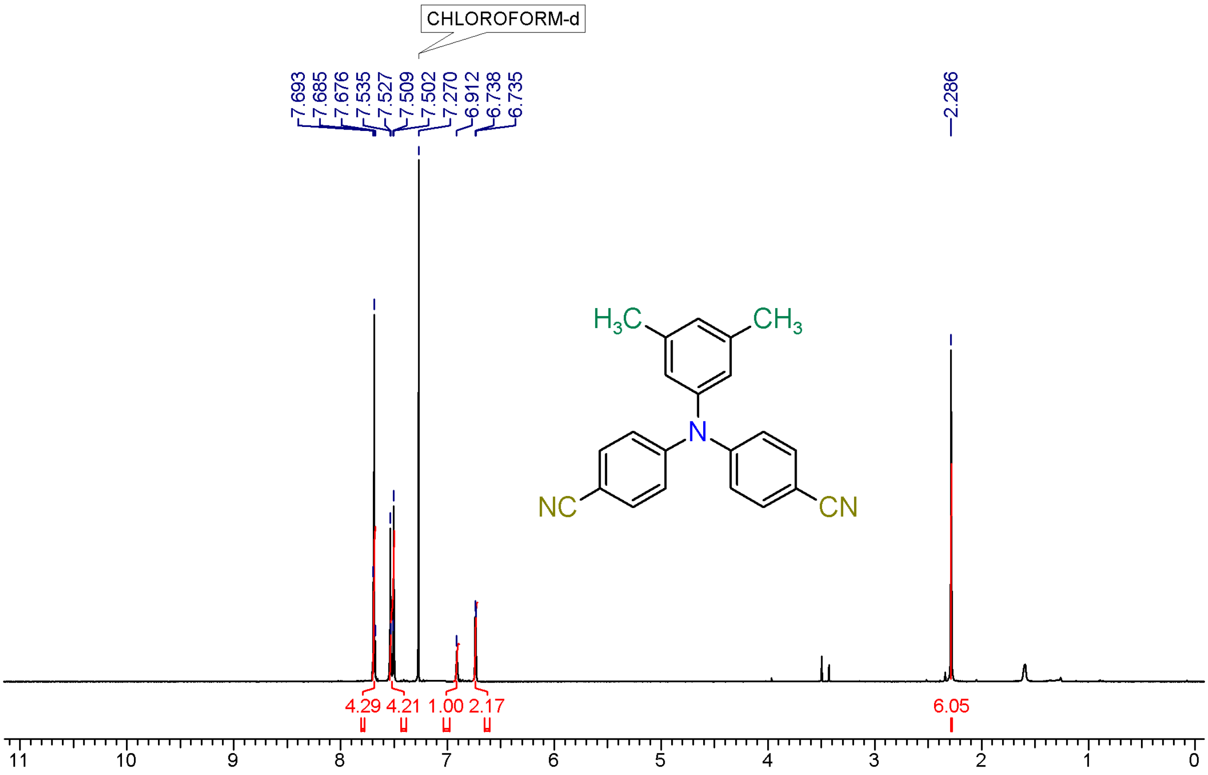

Figure S10: ^{1}H NMR of building block L_1.

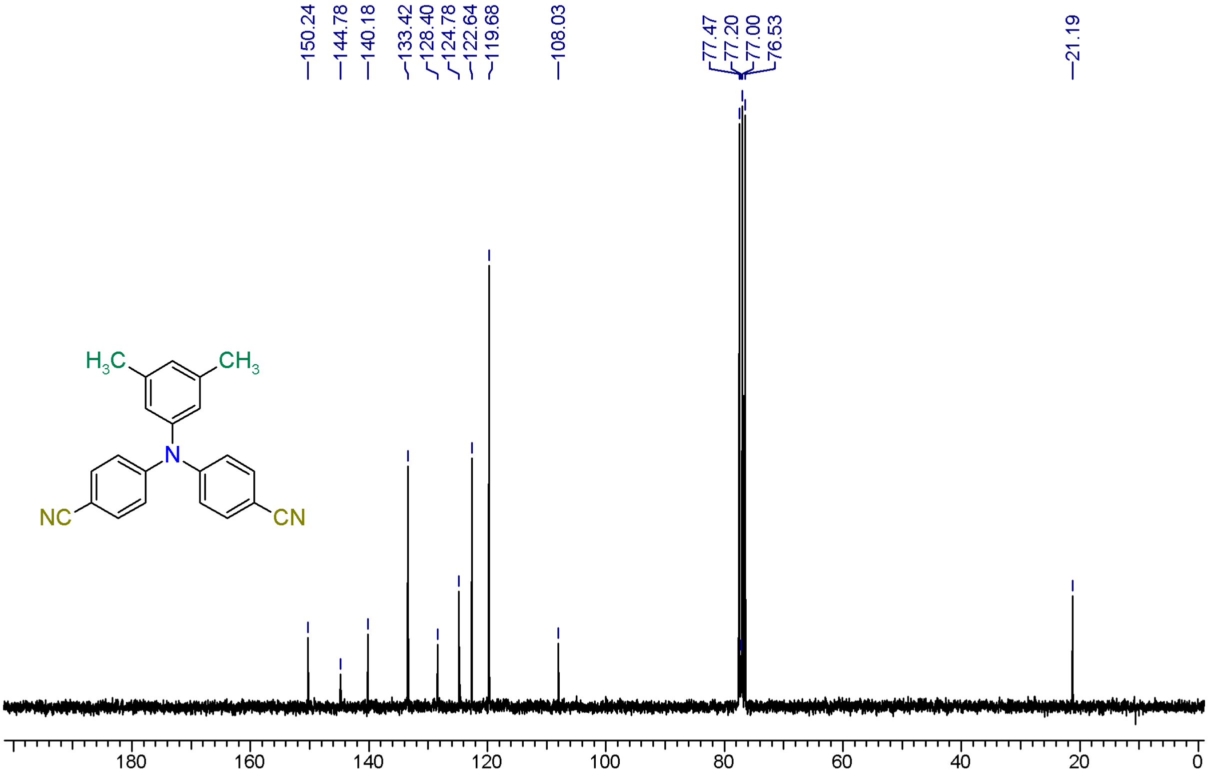

Figure S11: ^{13}C NMR of building block L_1.

Synthesis of Building Block L_2:

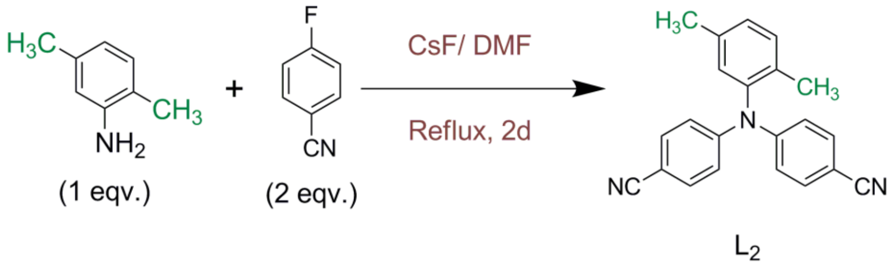

Figure S12: Synthesis protocol for the building block L_2.

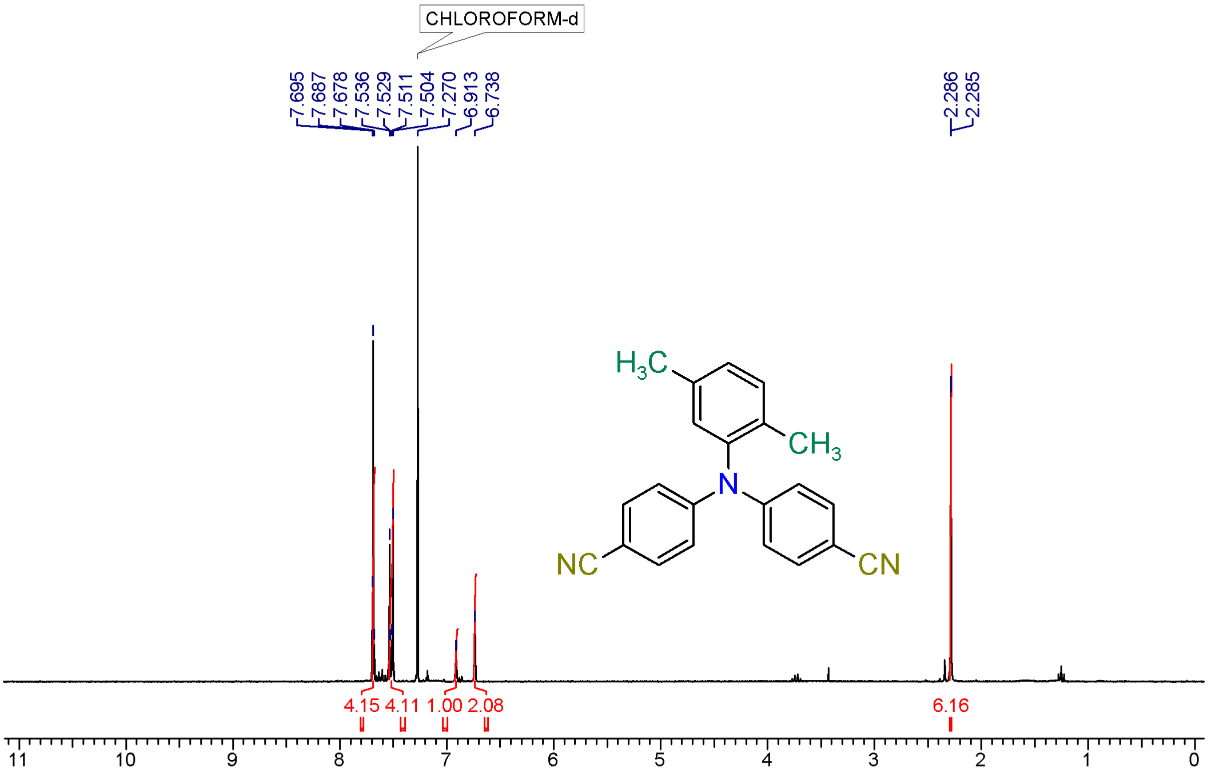

Figure S13: ^{1}H NMR of building block L_2.

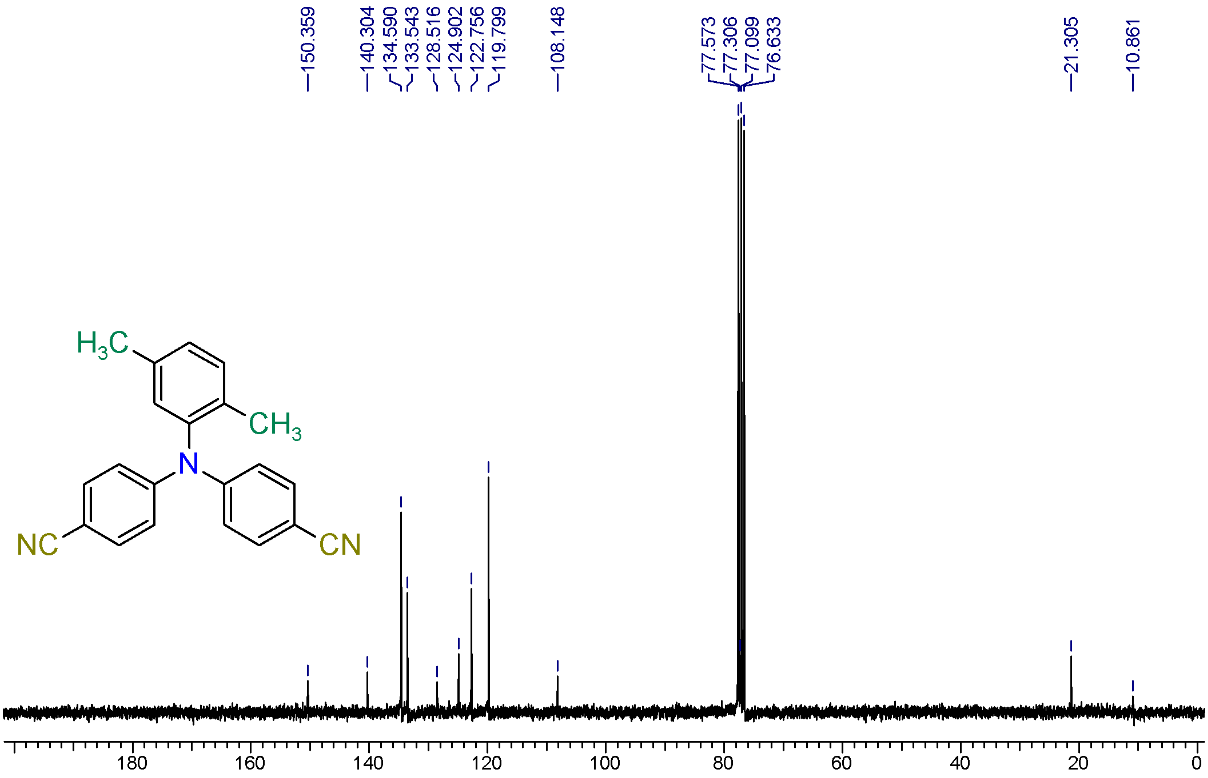

Figure S14: ^{13}C NMR of building block L_2.

Synthesis of Building Block L_3:

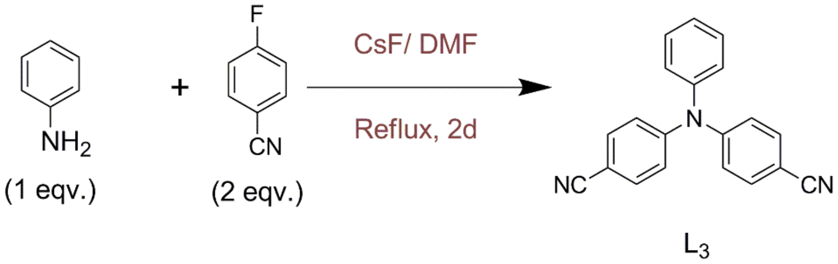

Figure S15: Synthesis protocol for the building block L_3.

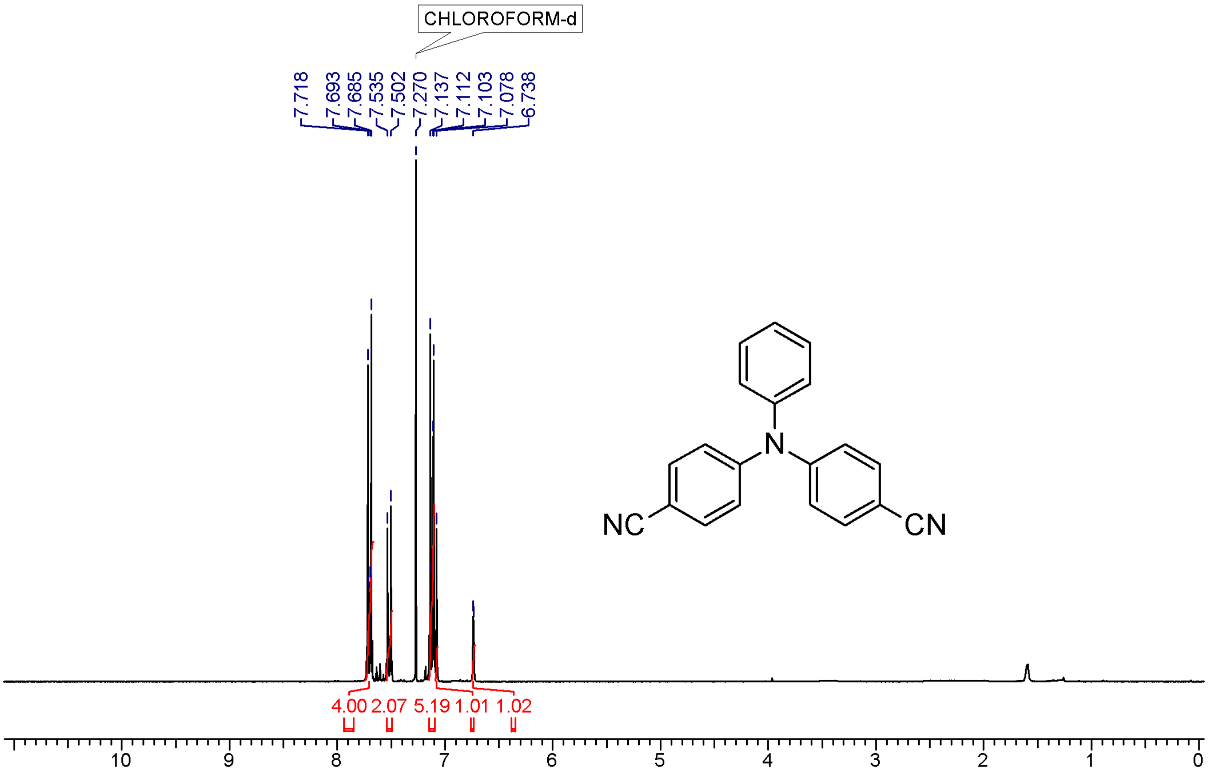

Figure S16: ^{1}H NMR of building block L_3.

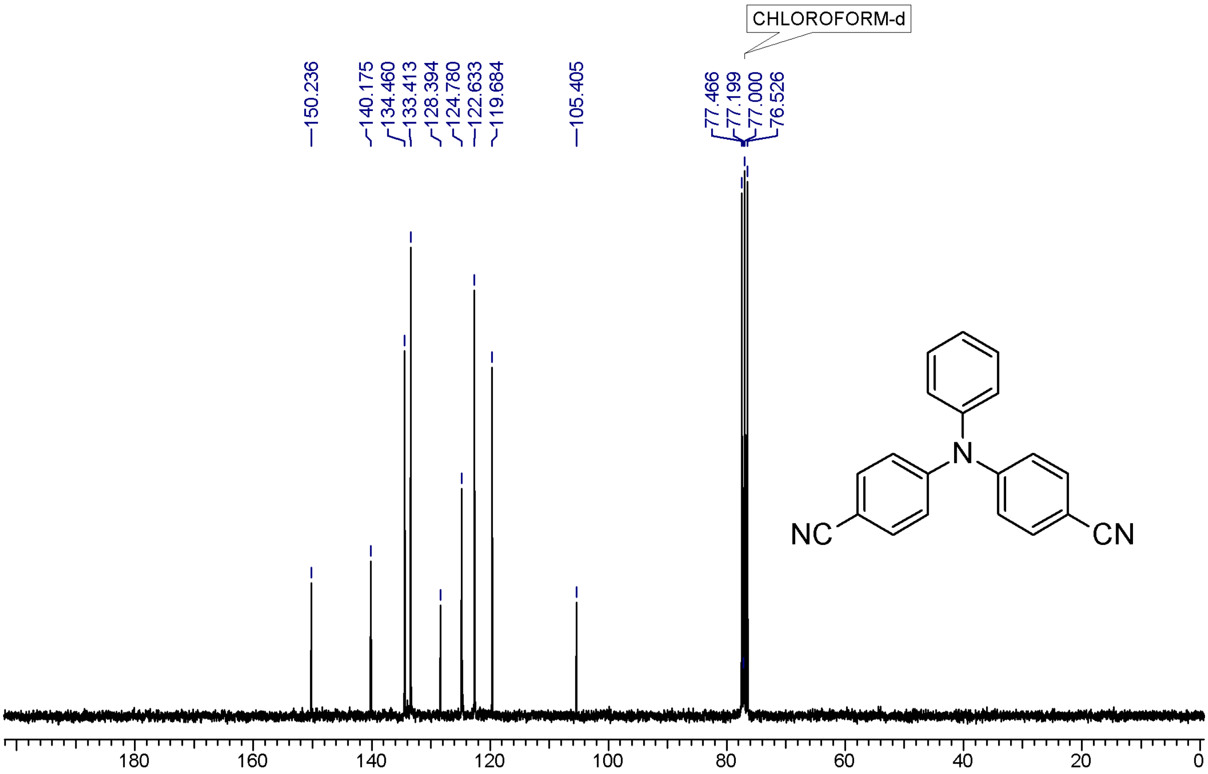

Figure S17: ^{13}C NMR of building block L_3.

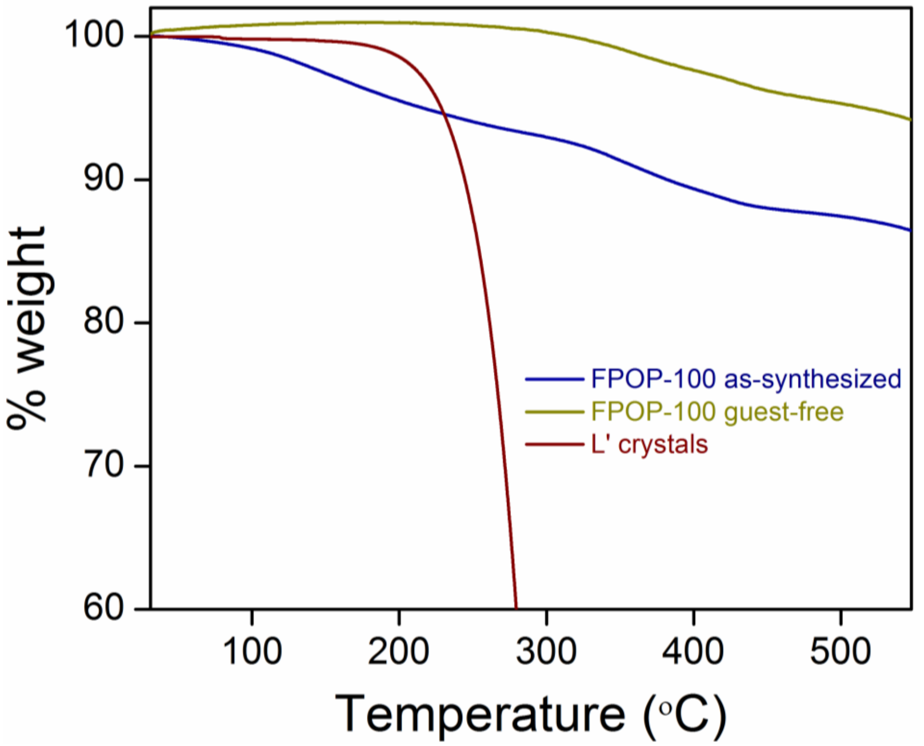

Figure S18: Thermogravimetric analysis (TGA) profile for **FPOP-100** (as-synthesized and desolvated phases), plotted along with the precursor crystals of dinitrile L'.

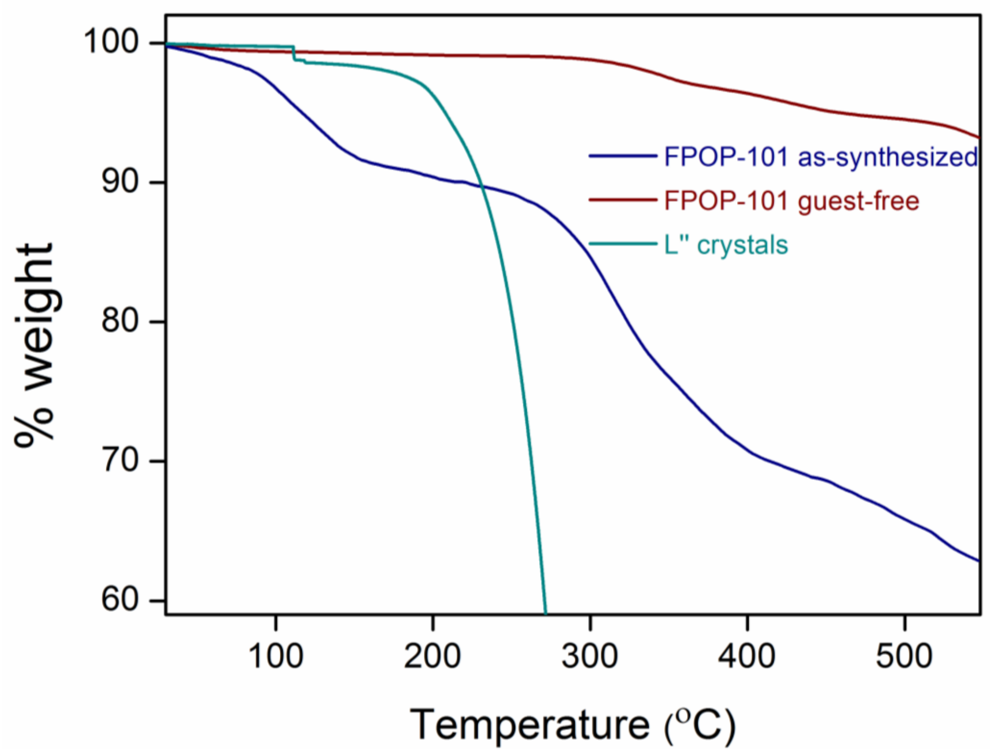

Figure S19: Thermogravimetric analysis (TGA) profile for **FPOP-101** (as-synthesized and desolvated phases), plotted along with the precursor crystals of dinitrile L''.

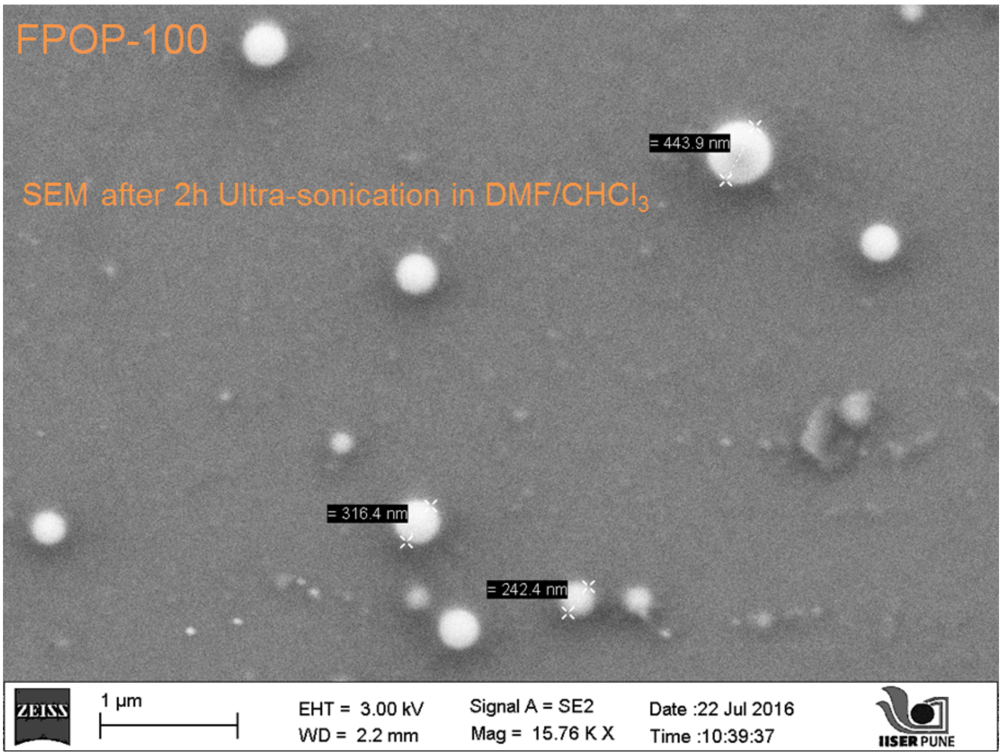

Figure S20: FE-SEM image for the DMF/$CHCl_3$-dispersed phase of **FPOP-100**.

.

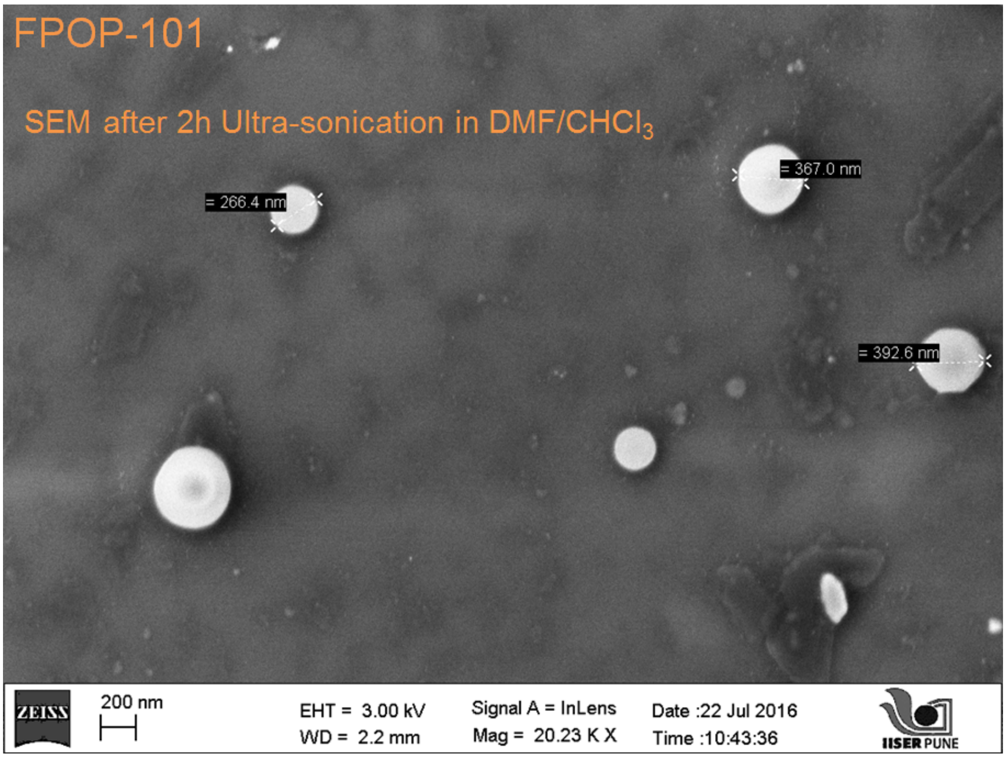

Figure S21: FE-SEM image for the DMF/$CHCl_3$-dispersed phase of **FPOP-101**.

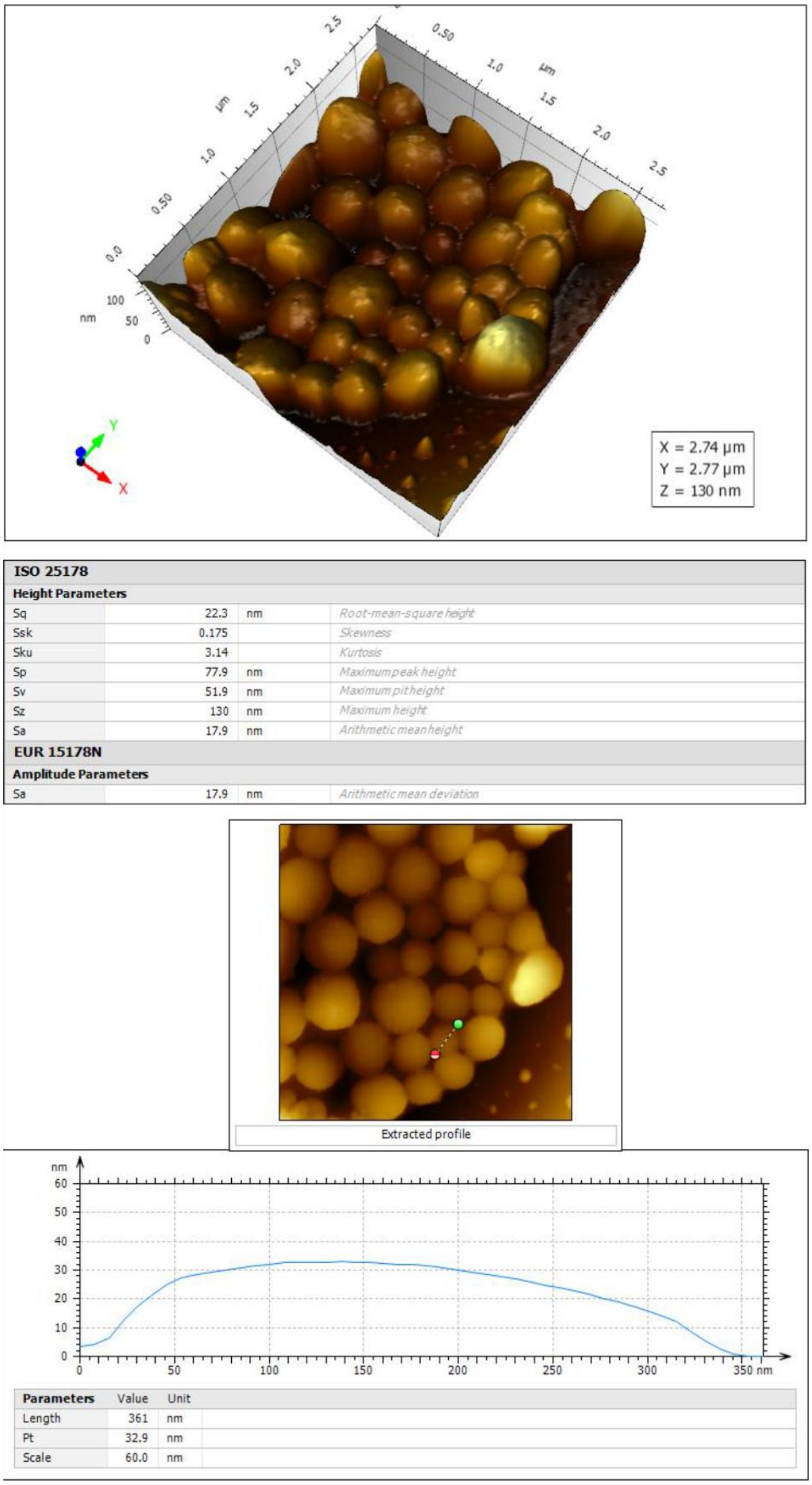

ISO 25178			
Height Parameters			
Sq	22.3	nm	*Root-mean-square height*
Ssk	0.175		*Skewness*
Sku	3.14		*Kurtosis*
Sp	77.9	nm	*Maximum peak height*
Sv	51.9	nm	*Maximum pit height*
Sz	130	nm	*Maximum height*
Sa	17.9	nm	*Arithmetic mean height*
EUR 15178N			
Amplitude Parameters			
Sa	17.9	nm	*Arithmetic mean deviation*

Parameters	Value	Unit
Length	361	nm
Pt	32.9	nm
Scale	60.0	nm

Figure S22: AFM images for **FPOP-100**.

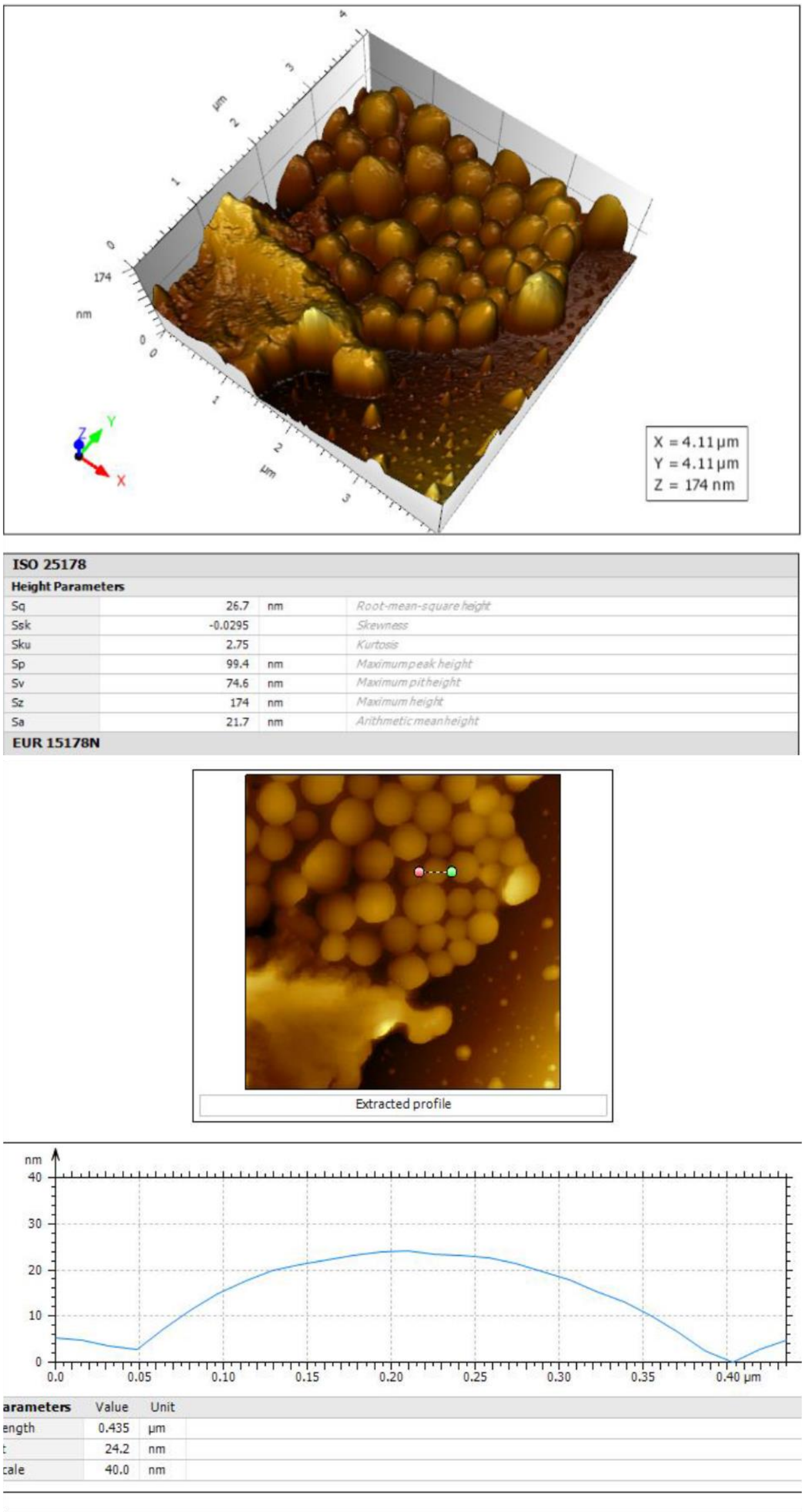

ISO 25178

Height Parameters

Sq	26.7	nm	*Root-mean-square height*
Ssk	-0.0295		*Skewness*
Sku	2.75		*Kurtosis*
Sp	99.4	nm	*Maximum peak height*
Sv	74.6	nm	*Maximum pit height*
Sz	174	nm	*Maximum height*
Sa	21.7	nm	*Arithmetic mean height*

EUR 15178N

arameters	Value	Unit
ength	0.435	µm
t	24.2	nm
cale	40.0	nm

Figure S23: AFM images for **FPOP-101**.

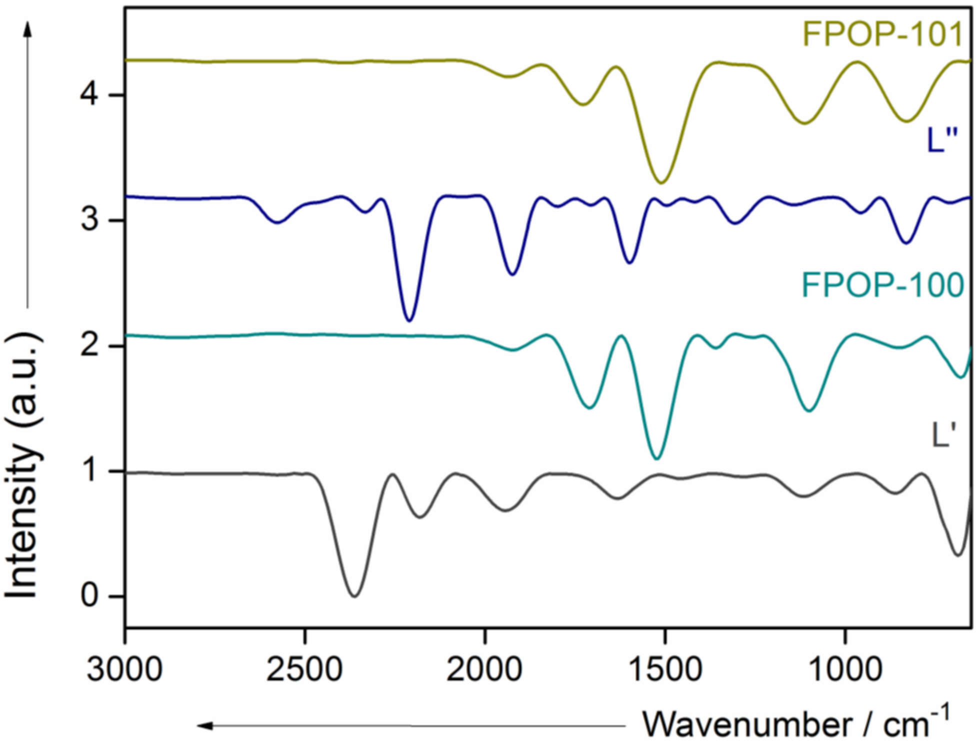

Figure S24: FT-IR spectral data recorded for a) L', b) **FPOP-100**, c) L" and **FPOP-101** (stacked together).

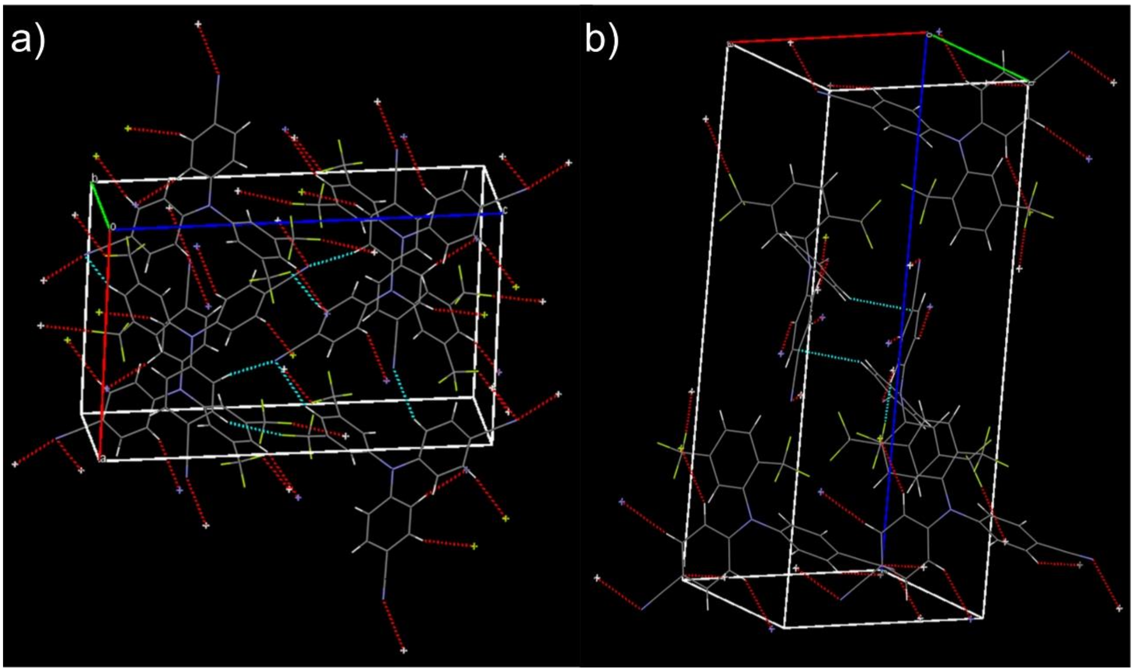

Figure S25: Manifold modes of intermolecular H-bonding and van der Waals interactions observed in the single crystal structures for the precursors L' and L" (considering one unit cell for each of the precursors).

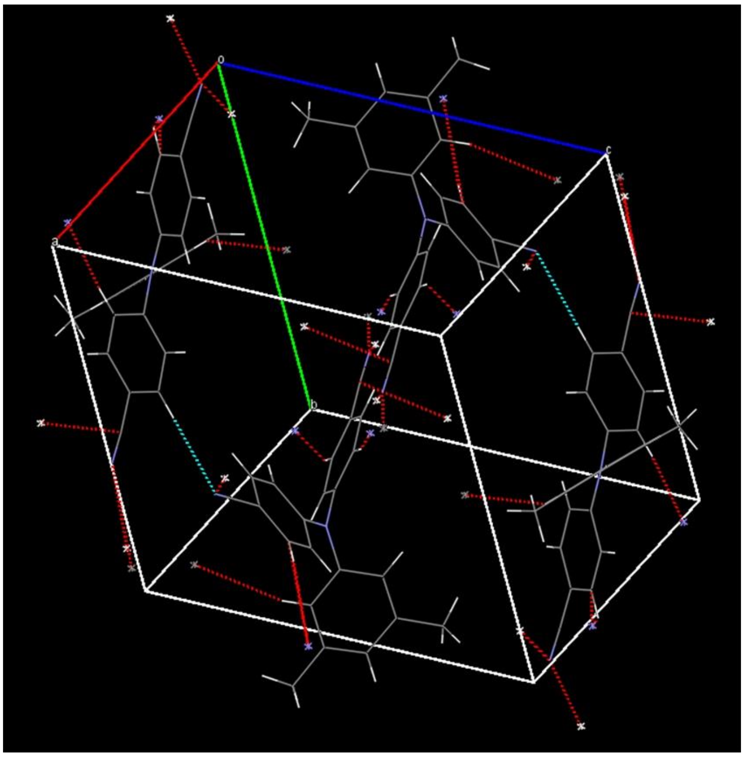

Figure S26: Single mode of intermolecular H-bonding and van der Waals interactions observed in the single crystal structure of the precursor L_1 (considering one unit cell).

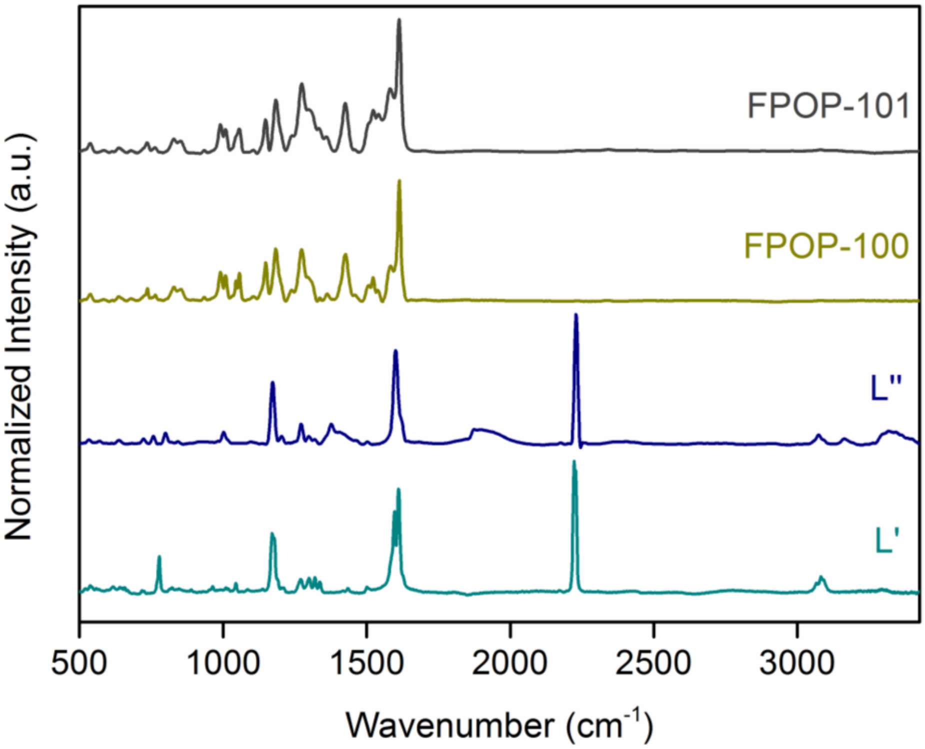

Figure S27: Comparison of Raman spectra for the dinitrile precursors (L', L"), and the corresponding POPs viz. **FPOP-100** and **FPOP-101**, respectively.

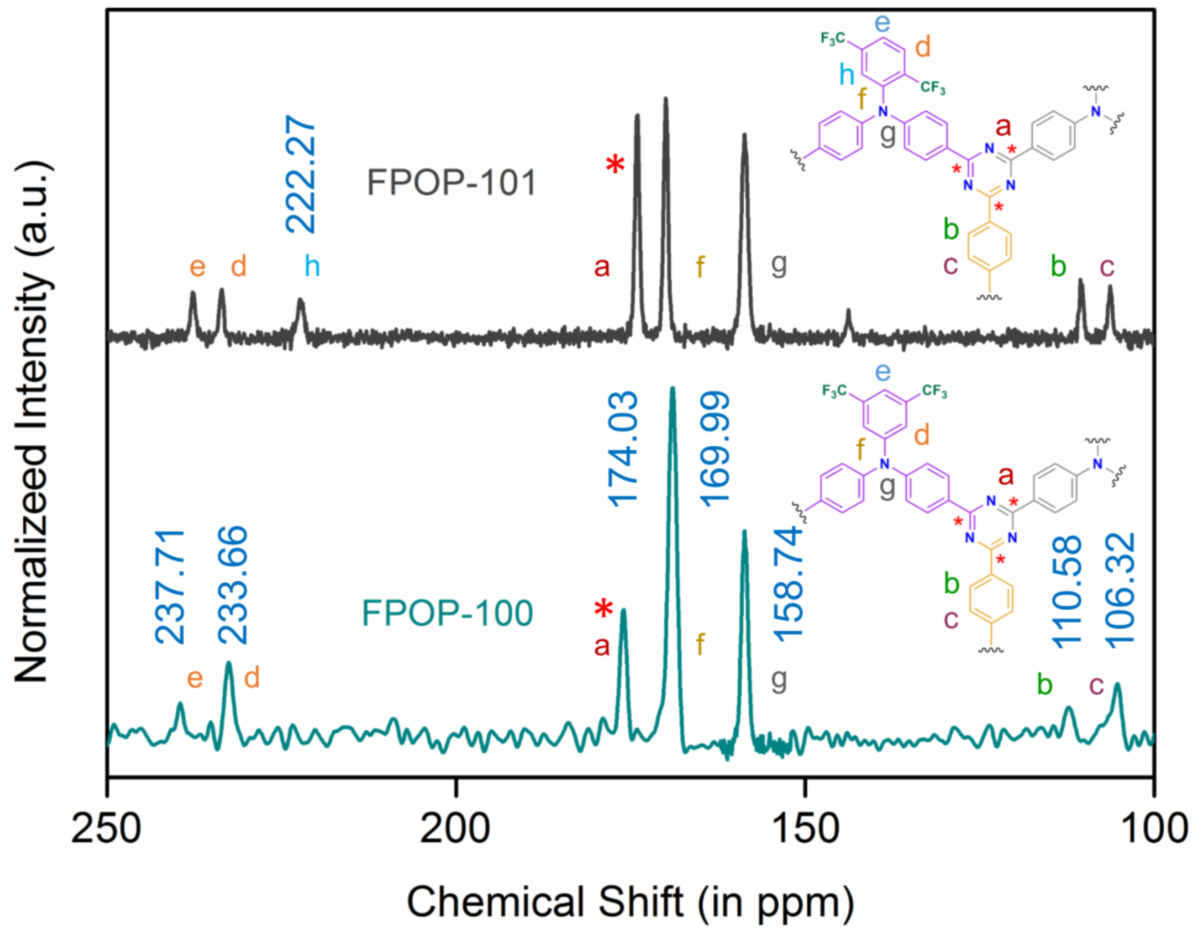

Figure S28: ^{13}C CP-MAS SSNMR for the two guest-free POPs, *viz.* **FPOP-100** and **FPOP-101**, respectively. The asterisks denote the peaks corresponding to the triazine ring carbon atoms (a), while the other six peaks correspond to other aromatic carbon atoms (b-g for **FPOP-100** and b-h for **FPOP-101**); most downfield ‘d’, ‘e’, and ‘h’-labeled carbons lead to the highest δ values (> 200 ppm). The isotopic peak positions at frequencies > 200 ppm indicates to a possibility that the SSNMR setup might need be referenced further to TMS (or DSS) for setting up an useful zero.

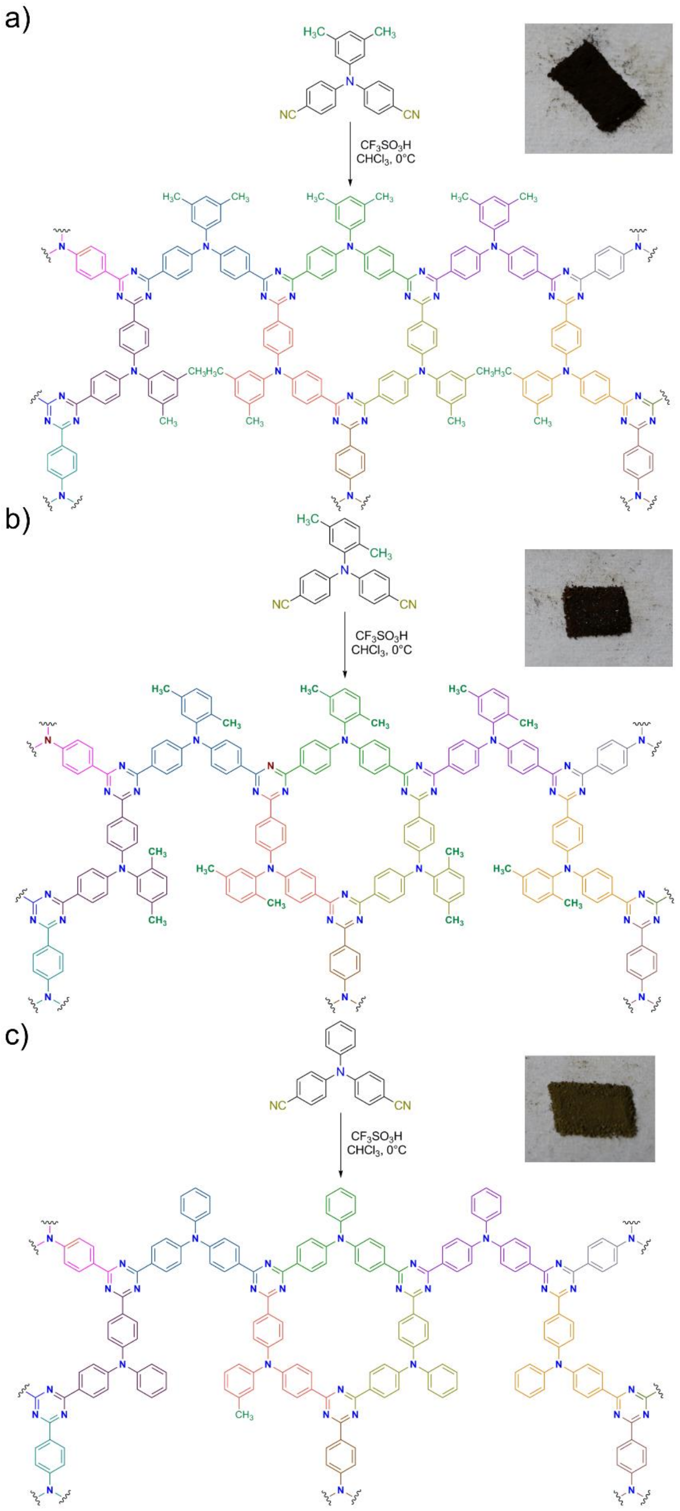

Figure S29: Schematic representations for the syntheses of POPs: a) **MPOP-100**, b) **MPOP-101**, and c) **POP-100**; Insets show the mechanically ductile/malleable texture for compounds **MPOP-100**, **MPOP-101** and **POP-100**.

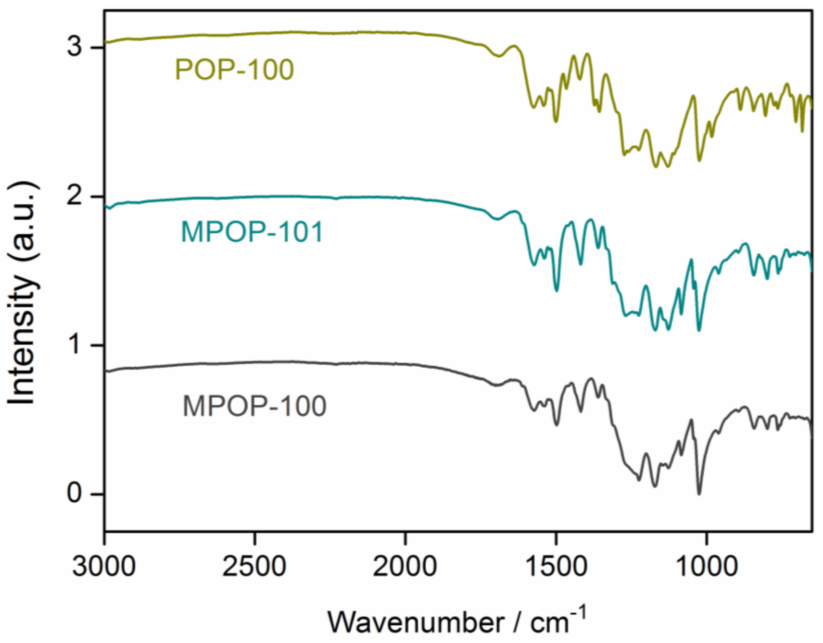

Figure S30: FT-IR spectral data-sets recorded for a) **MPOP-100**, b) **MPOP-101**, and c) **POP-100** (stacked together as Y-axis offsets).

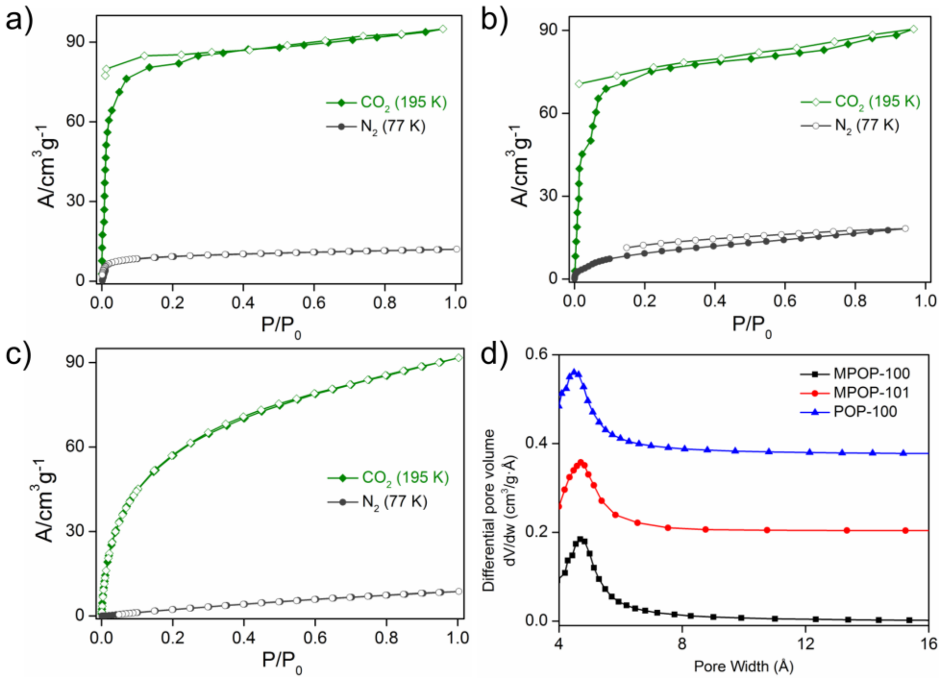

Figure S31. Low temperature CO_2 and N_2 adsorption isotherms for a) **MPOP-100**, b) **MPOP-101**, and c) **POP-100**, filled and empty symbols represent adsorption and desorption; d) Horvath-Kawazoe (H-K) pore size distribution profiles for the MPOP pair with **POP-100**, calculated from CO_2 isotherms at 195 K.

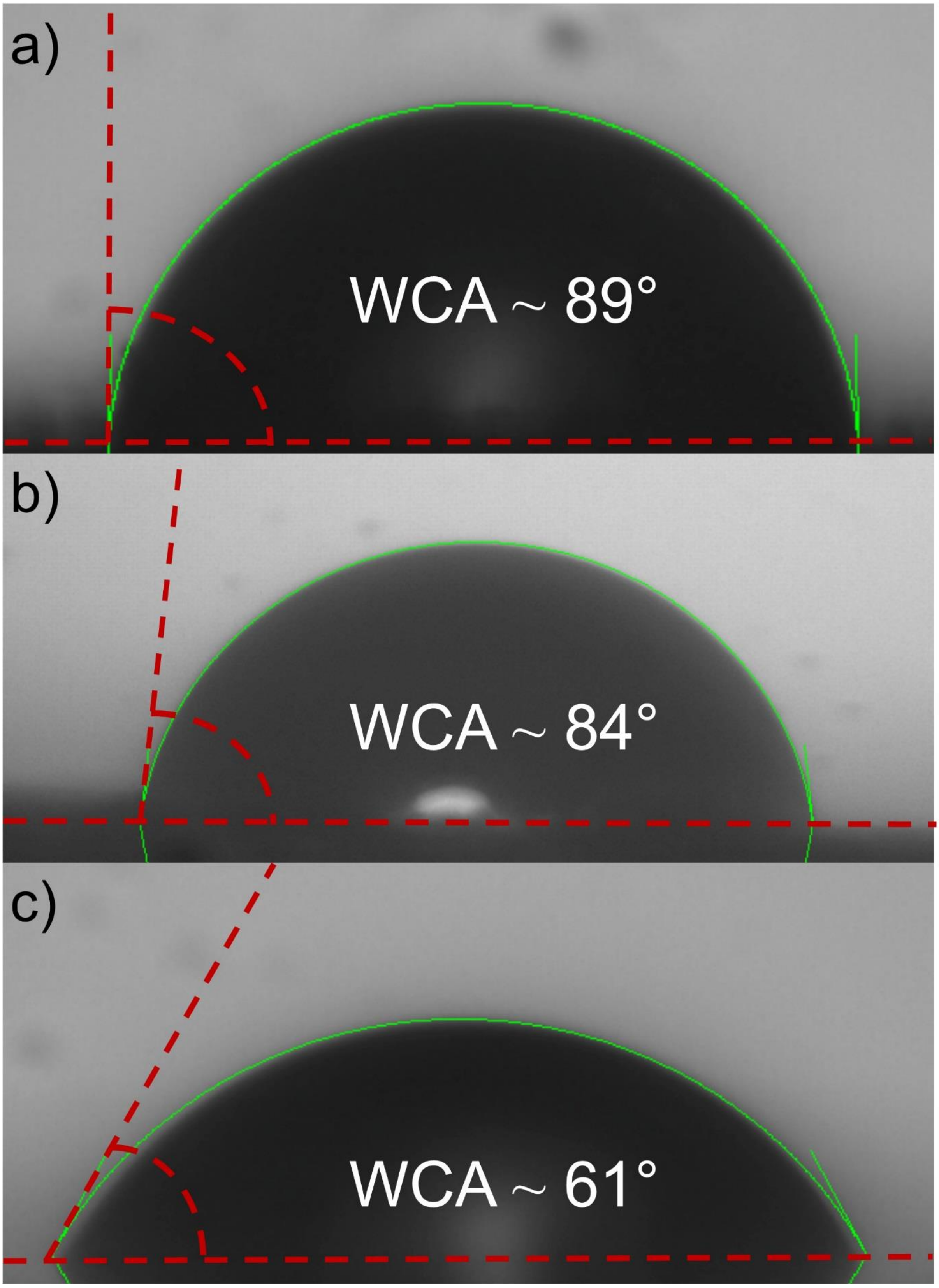

Figure S32: Water contact angles measured on a) **MPOP-100**, b) **MPOP-101**, c) **POP-100** compound pellets.

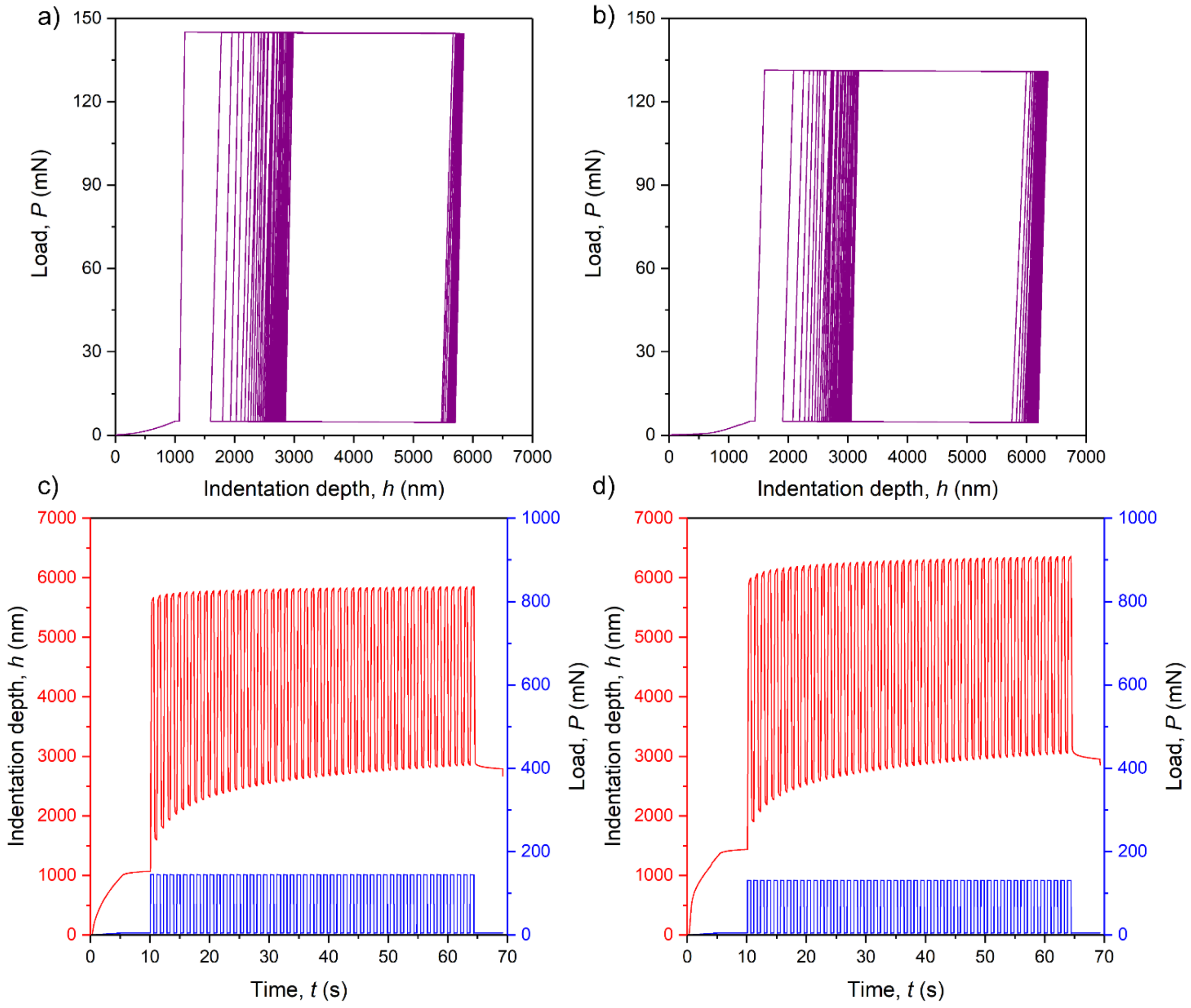

Figure S33. Loading scheme of the cyclic impact tests on **FPOP-100** and -101. Load vs indentation depth for a) **FPOP-100**, b) **FPOP-101**. Time evolution of Indentation depth and load for c) **FPOP-100**, d) **FPOP-101**. **FPOP-101** seems to be less harder than **FPOP-100** according to a) & b). A plausible explanation is that fracture of **FPOP-101** is serverer than **FPOP-100** (see Fig. 7) given the load in impact test is about 8 times as high as the one in individual MTS indentations (as shown in Fig. 4a).

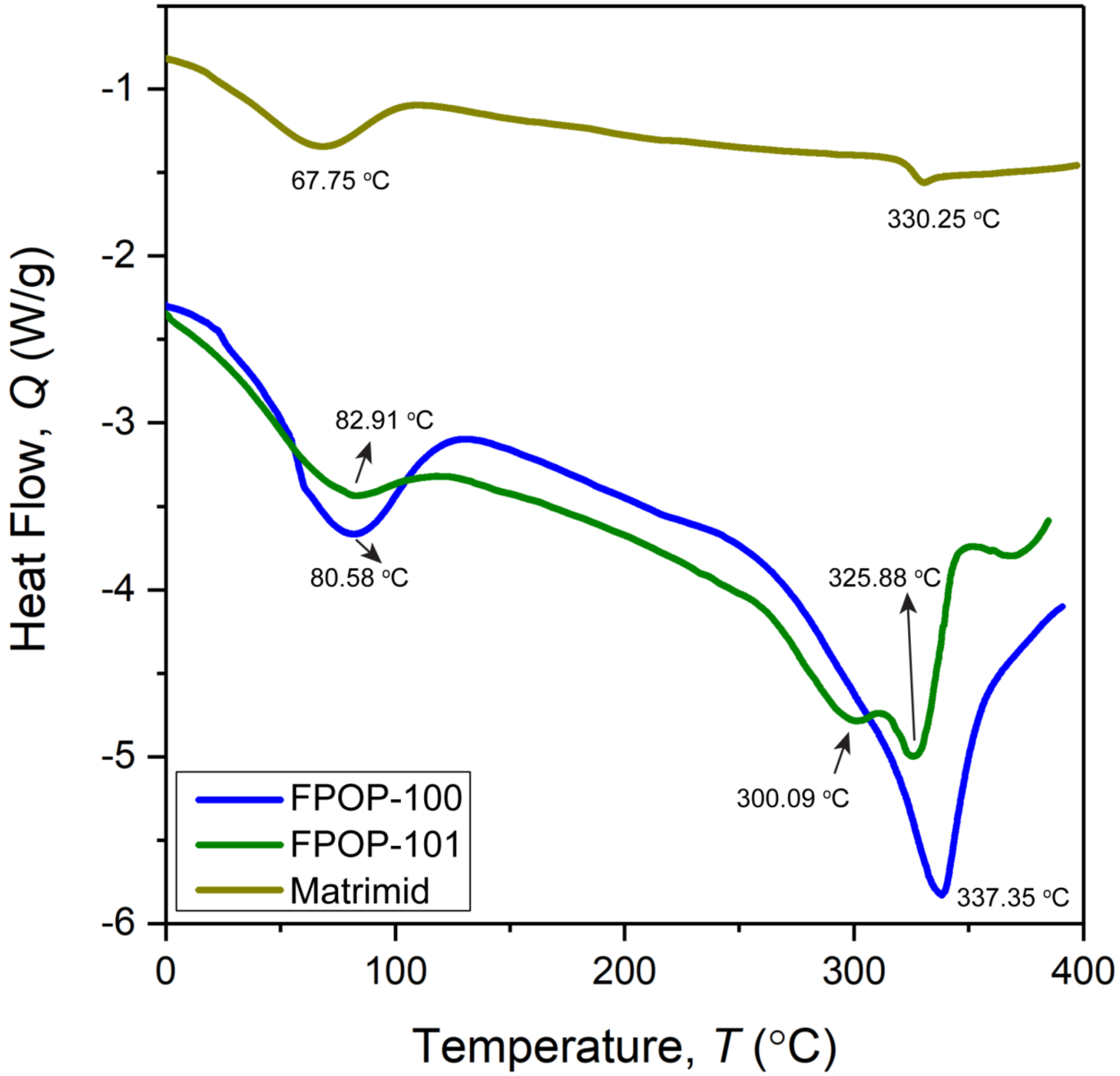

Figure S34. Differential scanning calorimetry of **FPOP**s and matrimid (polymer acts as a reference). **FPOP-100** at 80.58 °C and **FPOP-101** at 82.91 °C might undergo secondary relaxation (*β*) that is deduced by the similar behavior of Matrimid.[[1]] Transition temperature 300.09 °C for **FPOP-101** might originate from a recrystallization process, while the temperatures 337.35 °C for **FPOP-100** and 325.88 °C of **FPOP-101** could be the corresponding glass transition temperatures.

[1] E. M. Mahdi, J.-C. Tan, *J Memb. Sci.* **2016**, *498*, 276-290.